Predicting Atlantic Basin Seasonal Tropical Cyclone Activity by 1 June

WILLIAM M. GRAY AND CHRISTOPHER W. LANDSEA

Department of Atmospheric Science, Colorado State University, Fort Collins, Colorado

PAUL W. MIELKE JR., AND KENNETH J. BERRY

Department of Statistics, Colorado State University, Fort Collins, Colorado

(Manuscript received 1 April 1993, in final form 9 September 1993)

ABSTRACT

This is the third in a series of papers describing the potential for the seasonal forecasting of Atlantic basin tropical cyclone activity. Earlier papers by the authors describe seasonal prediction from 1 December of the previous year and from 1 August of the current year; this work demonstrates the degree of predictability by 1 June, the "official" beginning of the hurricane season. Through three groupings consisting of 13 separate predictors, hindcasts are made that explain 51%–72% of the variability as measured by cross-validated agreement coefficients for eight measures of seasonal tropical cyclone activity. The three groupings of predictors include 1) an extrapolation of quasi-biennial oscillation of 50- and 30-mb zonal winds and the vertical shear between the 50- and 30-mb zonal winds (three predictors); 2) West African rainfall, sea level pressure, and temperature data (four predictors); and 3) Caribbean basin and El Niño–Southern Oscillation information including Caribbean 200-mb zonal winds and sea level pressures, equatorial eastern Pacific sea surface temperatures and Southern Oscillation index values, and their changes in time (six predictors). The cross validation is carried out using least sum of absolute deviations regression that provides an efficient procedure for the maximum agreement measure criterion. Corrected intense hurricane data for the 1950s and 1960s have been incorporated into the forecasts. Comparisons of these 1 June forecast results with forecast results from 1 December of the year previous and 1 August of the current year are also given.

1. Introduction

This paper describes an empirically based statistical forecasting scheme for seasonal prediction of Atlantic basin tropical cyclone activity by 1 June, the "official" beginning of the hurricane season. Earlier papers by the authors have shown skillful seasonal forecasting by 1 December of the previous year (Gray et al. 1992a) and by 1 August of the current year (Gray et al. 1993). The results presented here build upon this previous work and provide improved forecasts using additional predictors that are available by the end of May.

Thirteen variables are arranged into three predictor groupings. The groupings include 1) stratospheric quasi-biennial oscillation (QBO) data, 2) West African surface data, and 3) Caribbean basin/El Niño–Southern Oscillation (ENSO) information. The stratospheric QBO group is composed of 50- and 30-mb zonal winds and the absolute value of the vertical wind shear between the two levels extrapolated from May to September near 10°N. The West African surface data grouping is composed of previous year August–November Gulf of Guinea rainfall, previous year August–September western Sahelian rainfall, current year February–May West African east to west sea level pressure gradients, and current year February–May West African east to west temperature gradients. The Caribbean basin–ENSO factors include the April and May conditions of the equatorial eastern Pacific sea surface temperature (SST) anomalies, and the standardized Tahiti minus Darwin sea level pressure index (i.e., the Southern Oscillation index or SOI), the time change of these quantities from January and February to April and May, and the 200-mb zonal wind anomalies (ZWA) and the sea level pressure anomalies (SLPA) within the Caribbean basin for April and May.

The tropical cyclone–dependent variables include the seasonal total numbers of named storms (NS), hurricanes (H), intense (or major) hurricanes (IH), named storm days (NSD), hurricane days (HD), intense hurricane days (IHD), and hurricane destruction potential (HDP). Definitions of these are contained in Gray et al. (1992a, 1993) and Landsea (1993). Also included is a new parameter of seasonal activity termed the net tropical cyclone activity (NTC), which is defined as

Corresponding author address: Dr. William M. Gray, Department of Atmospheric Science, Colorado State University, Fort Collins, CO 80523.

TABLE 1. Summary of Atlantic tropical cyclone data for the years 1950–1991 with updated data from Neumann et al. (1987) and Jarvinen et al. (1984). The numbered columns indicate the seasonal total of NS (named storms), NSD (named storm days), H (hurricanes), HD (hurricane days), IH* (intense or major hurricanes), IHD* (intense hurricane days), HDP* (hurricane destruction potential), and NTC* (net tropical cyclone activity). Note that the data with an asterisk are bias-corrected values following the analysis of Landsea (1993).

Year	NS	NSD	H	HD	IH*	IHD*	HDP*	NTC*
1950	13	98	11	60	7	15.75	200	243
1951	10	58	8	36	2	5.00	113	121
1952	7	40	6	23	3	3.75	70	97
1953	14	64	6	18	3	5.50	59	121
1954	11	44	8	32	2	8.50	91	127
1955	12	82	9	47	5	13.75	158	198
1956	8	30	4	13	2	2.25	39	69
1957	8	38	3	21	2	5.25	66	86
1958	10	56	7	30	4	8.25	94	140
1959	11	41	7	22	2	3.75	60	99
1960	7	30	4	18	2	10.75	72	101
1961	11	71	8	48	6	20.75	170	222
1962	5	22	3	11	0	0.00	26	33
1963	9	52	7	37	2	5.50	103	116
1964	12	71	6	43	5	9.75	139	168
1965	6	40	4	27	1	6.25	73	86
1966	11	62	7	42	3	7.00	121	140
1967	8	58	6	36	1	3.25	98	97
1968	7	26	4	10	0	0.00	18	41
1969	17	84	12	40	3	2.75	110	157
1970	10	24	5	7	2	1.00	18	65
1971	13	63	6	29	1	1.00	65	95
1972	4	21	3	6	0	0.00	14	28
1973	7	33	4	10	1	0.25	24	52
1974	7	32	4	14	2	4.25	46	76
1975	8	43	6	20	3	2.25	54	92
1976	8	45	6	26	2	1.00	65	85
1977	6	14	5	7	1	1.00	18	46
1978	11	40	5	14	2	3.50	40	86
1979	8	44	5	22	2	5.75	73	96
1980	11	60	9	38	2	7.25	126	135
1981	11	61	7	22	3	3.75	63	114
1982	5	16	2	6	1	1.25	18	37
1983	4	14	3	4	1	0.25	8	32
1984	12	51	5	18	1	0.75	42	77
1985	11	51	7	21	3	4.00	61	110
1986	6	23	4	10	0	0.00	23	38
1987	7	37	3	5	1	0.50	11	48
1988	12	47	5	24	3	8.00	81	121
1989	11	66	7	32	2	10.75	108	140
1990	14	68	8	28	1	1.00	57	104
1991	8	22	4	8	2	1.25	23	59

$$\mathrm{NTC} = (\%\mathrm{NS} + \%\mathrm{H} + \%\mathrm{IH} + \%\mathrm{NSD} + \%\mathrm{HD} + \%\mathrm{IHD})/6,$$

where each season's percentage value from the long period mean is used for the six measures of seasonal activity. The NTC value is useful as a seasonal tropical cyclone measure because it combines most of the other tropical cyclone parameters of interest into a single measure of activity. There are many seasons in which a single parameter, such as a number of hurricanes, is not representative of the entire tropical cyclone activity of that year. For instance, 1977 had 5 H, but was otherwise an inactive year: only 7 HD, 1 IH, and 1 IHD. By contrast, while 1988 also had 5 H, other seasonal parameters indicated an active year: 24 HD, 3 IH, and 8 IHD. These are examples of years having an identical parameter yet much different levels of other activity. To overcome these difficulties we propose the use of a single index, which is a combination of six measures of tropical cyclone activity.

Note that the 1950–1969 quantities of IH, IHD, HDP, and NTC have been adjusted to reflect a small overestimation of tropical cyclone intensities as reported by Landsea (1993). These values, which are slightly reduced from previously published data (Gray et al. 1992a, 1993), are identified as IH*, IHD*, HDP*, and NTC*. Table 1 shows the individual yearly values for each dependent variable.

This report will briefly discuss the predictors that have been previously used as well as a more in-depth

look at two new predictors that are the West African east–west sea level pressure and temperature gradients. Analyses of hindcasts based on the years 1950–1991 are presented, and a comparison with previous results is made. Note that years before 1950 are not available for hindcast use because of a lack of stratospheric data. Finally, implications of the results and possibilities of future improvements are discussed in the last section.

2. Predictors of Atlantic tropical cyclone activity

a. Previously identified predictors

Early work by the lead author (Gray 1984a,b) indicated that Atlantic tropical cyclone activity had a seasonal dependence to pre–1 June values of Caribbean basin SLPA and ZWA as well as to the phase of the stratospheric QBO and whether or not a warm ENSO event was in progress. More recent studies have also identified previous year rainfall occurring over West Africa as a strong predictor of future tropical cyclone activity (Gray et al. 1992a). What follows is a brief review of these predictors and how they appear to be related to tropical cyclone activity.

Stratospheric quasi-biennial oscillation (QBO). Gray (1984a) and Shapiro (1989) have recognized that the stratospheric QBO apparently modulates Atlantic basin tropical cyclone activity: suppressed conditions tend to occur during QBO east phases, while enhanced tropical cyclone activity is typically observed during QBO west phases. More recently, Gray et al. (1992a, 1993) have also used the vertical shear between 50- and 30-mb zonal winds as a predictor of tropical cyclone activity, whereby small amounts of shear increase the number of storms and large amounts of shear decrease the number of storms. Current research (Gray et al. 1992b, 1993; Knaff 1993) suggests that the physical mechanisms relating tropical convection (and tropical cyclones) to the stratospheric QBO are associated with upper-tropospheric to lower-stratospheric vertical wind shear as well as systematic height field differences in the upper troposphere. QBO east phase conditions favor equatorial (0°–7° latitude) convection over off-equatorial (8°–18°) convection. Conversely, in QBO west phase years, off-equatorial convection is enhanced, while equatorial convection is suppressed. Because of the very regular progression of the QBO cycle, it is possible to make skillful extrapolations of 50- and 30-mb zonal winds by simply knowing the current phase and magnitude of the QBO and projecting the values forward in time using past histories of the QBO as a guide (Gray et al. 1992a). Thus, using May data, we make a four-month extrapolation to September, the height of the hurricane season, of zonal winds near 10°N at 50 mb (U_{50}) and 30 mb (U_{30}), and the absolute shear between the two levels ($|U_{50} - U_{30}|$) at this latitude as shown in Table 2.

West African rainfall. Recently, it has been uncovered that there is a strong concurrent relationship between west Sahel rainfall and Atlantic basin tropical cyclone activity, especially IH activity (Gray 1990; Landsea and Gray 1992). Landsea et al. (1992) observed that this relationship has held since the beginning of this century. This association is hypothesized to be due to interannual variations in the upper-tropospheric flow patterns (e.g., a wet western Sahel and active tropical cyclone season are both related to easterly Caribbean basin and tropical Atlantic ZWA) and to easterly wave intensities (e.g., wet/active conditions also are related to a number of stronger-amplitude tropical waves originating over North Africa). Goldenberg and Shapiro (1993) have recently provided more evidence that tropospheric vertical shear is a dominant mechanism connecting the Sahelian monsoon rains and seasonal Atlantic basin tropical cyclones.

In addition to the concurrent relationships, two measures of rainfall in West Africa have been shown to provide a measure of seasonal western Sahel rainfall–Atlantic tropical cyclone activity with a multimonth lead time (Gray et al. 1992a). The first is rainfall that occurs along the Gulf of Guinea coast from August through November of the previous year. It is suggested that the moisture from this rainfall acts to enhance the following summer monsoon through evaporation/evapotranspiration. Thus, above-normal Gulf of Guinea rainfall allows for greater moisture storage, a later increase in evaporation/evapotranspiration, and an enhanced monsoon trough with more rain in the Sahel. The second predictor is rainfall that occurs in August and September throughout the western Sahel. Because of the strong year-to-year persistence that Sahel rainfall has experienced in the last four decades (Nicholson 1979), the use of previous year Sahel rainfall to forecast next year Sahel rain (and thus Atlantic hurricane activity) has a modest amount of skill. Both the Gulf of Guinea (R_g) and the west Sahel (R_s) rainfall anomalies are shown in Table 2.

Caribbean basin sea level pressure anomalies (SLPA). Stations located throughout the Caribbean basin show an inverse relationship of April and May sea level pressure to subsequent tropical cyclone activity. In general, higher pressure precedes quiet conditions, while lower pressure indicates more activity to come (Ray 1935; Brennan 1935; Shapiro 1982; Gray 1984b). Surface pressure variations are suggested to be associated with interannual fluctuations of the location and/or the intensity of the intertropical convergence zone (ITCZ). Lower pressure would indicate a farther poleward excursion than normal of the ITCZ and/or a stronger ITCZ (more low-level convergence and vorticity) favoring tropical cyclone genesis. It is presumed that anomalous conditions occurring in April and May have a tendency to persist through the main months of the hurricane season (August–October). Note that Shapiro (1982) also indicated that although local sea surface temperatures show a degree of pre-

TABLE 2. Data for the 13 predictors for each year from 1950 to 1991 used to make the 1 June forecast of subsequent Atlantic tropical cyclone activity. Note that data in columns 4, 5, 6, 7, 12, and 13 are expressed in terms of standardized deviations and that data in columns 8, 9, 10, and 11 are departures from the long-term (1950–1991) means.

	Four-month extrapolated			Previous	Previous	Feb–May	
	U_{50}	U_{30}	$\lvert U_{50} - U_{30} \rvert$	Aug–Sep	Aug–Nov		
	m s^{-1}	m s^{-1}	m s^{-1}	R_s	R_g	$\Delta_x P$	$\Delta_x T$
Year	1	2	3	4	5	6	7
1950	−3	−3	0	−0.12	1.09	0.52	1.55
1951	−4	−18	14	1.71	−0.65	0.81	−0.62
1952	−22	−26	4	0.52	0.67	1.47	−0.21
1953	−1	−18	17	0.96	0.42	1.30	−0.24
1954	−22	−30	8	0.23	−0.14	0.09	−0.28
1955	0	−8	8	0.63	0.66	1.71	0.75
1956	−20	−30	10	1.03	0.43	0.21	−1.25
1957	−2	−1	1	0.50	−0.34	0.58	0.62
1958	−12	−29	17	0.60	1.04	0.94	0.50
1959	−7	−1	6	1.48	−0.73	−0.17	−0.95
1960	−8	−30	22	0.27	0.13	0.90	0.81
1961	−3	−5	2	0.25	1.06	2.03	2.98
1962	−12	−30	18	0.50	−0.73	0.03	1.48
1963	−12	−1	11	0.30	0.75	0.18	0.68
1964	−4	−12	8	−0.10	1.20	0.25	1.16
1965	−17	−31	14	0.62	−0.66	−0.07	0.76
1966	−7	−1	6	0.78	−0.16	0.56	1.34
1967	−8	−26	18	0.36	−0.13	−0.50	−0.32
1968	−22	−14	8	0.75	−0.49	−0.60	−0.43
1969	−2	−2	0	−0.81	1.30	0.22	0.27
1970	−12	−31	19	0.40	−0.29	0.27	0.64
1971	−3	−3	0	−0.44	−0.21	−1.16	−1.77
1972	−12	−30	18	−0.17	−0.38	−1.15	−1.18
1973	−1	−5	4	−1.09	−0.87	−0.52	−0.80
1974	−14	−31	17	−0.71	0.45	−1.20	−0.92
1975	−7	−1	6	−0.02	−0.06	−1.14	−0.09
1976	−6	−26	20	0.08	−0.54	−1.62	−0.23
1977	−21	−14	7	−0.48	−0.58	0.01	1.22
1978	−1	−12	11	−0.73	−0.49	−0.41	−0.23
1979	−17	−31	14	−0.34	−0.71	−0.58	0.49
1980	−5	−2	3	−0.90	0.57	−0.88	−0.43
1981	−12	−29	17	−0.32	0.38	−0.21	0.33
1982	−18	−1	17	−0.42	−0.91	−1.10	−0.81
1983	−2	−18	16	−0.89	−0.60	0.13	0.26
1984	−20	−14	6	−1.22	−1.31	−0.07	−0.10
1985	−1	−7	6	−1.21	0.06	−0.47	−0.83
1986	−14	−28	14	−0.50	0.14	−1.82	−1.61
1987	−21	−3	18	0.02	−0.48	0.12	−0.37
1988	−3	−18	15	−0.61	1.39	−0.21	−0.55
1989	−21	−31	10	0.44	0.36	0.29	0.51
1990	−2	−2	0	0.15	0.20	0.54	1.65
1991	−12	−29	17	−0.79	−0.57	−1.34	−1.16

	Apr–May					
	SLPA	ZWA	Apr–May SST	(Apr–May)–(Jan–Feb) Δ_tSST	Apr–May SOI	(Apr–May)–(Jan–Feb) Δ_tSOI
	mb	m s^{-1}	10^{-2} °C	10^{-2} °C	10^{-1}	10^{-1}
Year	8	9	10	11	12	13
1950	−0.3	1.5	−93	41	10.8	0.0
1951	−0.2	1.5	34	64	−9.5	−18.7
1952	−0.2	−2.5	26	−43	0.5	9.0
1953	−0.3	−0.5	83	48	−13.2	−10.4
1954	−0.1	−1.5	−99	−106	4.5	4.6
1955	−0.1	0.0	−84	−42	3.1	−1.4
1956	−0.2	−0.5	−62	47	12.6	1.1
1957	0.4	1.2	83	112	−5.8	−6.5
1958	−1.2	−3.5	68	−55	−4.0	8.3
1959	0.0	0.0	34	−3	4.2	16.1
1960	−0.2	−2.5	5	12	6.0	6.7

TABLE 2. (*Continued*)

Year	Apr–May SLPA mb 8	Apr–May ZWA m s^{-1} 9	Apr–May SST 10^{-2} °C 10	(Apr–May)–(Jan–Feb) Δ_tSST 10^{-2} °C 11	Apr–May SOI 10^{-1} 12	(Apr–May)–(Jan–Feb) Δ_tSOI 10^{-1} 13
1961	0.7	−2.0	13	−2	4.9	3.6
1962	0.2	−3.7	−50	−28	5.7	0.0
1963	−0.1	0.0	20	60	4.9	−0.7
1964	0.3	0.4	−67	−106	4.1	7.3
1965	−0.3	4.0	58	84	−5.4	−3.7
1966	0.0	0.5	3	−100	−6.9	1.8
1967	0.3	2.1	−12	34	−2.9	−16.3
1968	0.6	1.8	−47	37	5.7	−0.7
1969	−1.2	−4.4	92	13	−6.9	4.0
1970	−0.2	−0.8	19	−63	−1.0	10.5
1971	0.2	0.5	−61	67	14.4	5.6
1972	0.0	1.5	68	88	−14.6	−19.8
1973	0.5	−4.4	−17	−147	0.5	9.8
1974	1.2	3.3	−53	70	10.0	−8.2
1975	0.4	1.3	−57	−2	9.3	9.9
1976	0.7	2.2	−33	93	1.6	−10.4
1977	0.5	0.9	12	−42	−8.8	−11.0
1978	−0.2	−1.3	−38	−76	4.2	19.5
1979	0.0	1.5	32	24	−0.3	−1.1
1980	0.1	0.2	46	−13	−7.2	−8.7
1981	−0.8	2.1	−24	−8	1.6	2.7
1982	0.2	3.4	48	35	−4.7	−9.0
1983	−1.1	2.5	145	−88	−5.0	28.6
1984	0.3	−2.5	3	23	0.8	−2.2
1985	0.3	0.3	−70	18	7.8	7.0
1986	−0.5	4.3	13	68	−2.5	−0.2
1987	−1.1	2.6	123	8	−21.6	−11.1
1988	0.0	−1.6	−78	−138	3.5	7.4
1989	0.9	1.6	−35	70	14.0	0.0
1990	−0.1	0.0	45	45	5.5	18.5
1991	0.5	4.2	60	40	−12.5	−15.0

dictive ability, they are essentially redundant to the information provided by SLPA. Table 2 shows the 1950–1991 values of April and May SLPA.

Caribbean basin 200-mb zonal wind anomalies (ZWA). Tropospheric vertical wind shear has long been recognized as a major inhibiting factor for tropical cyclogenesis and intensification (Gray 1968). Because of the circulation regime of the tropical North Atlantic, tropospheric vertical shear is dominated by the variations in the upper troposphere. Thus, with the nearly constant trade-wind flow (e.g., easterlies) near the surface, 200-mb ZWA adequately describe vertical wind shear: positive anomalies (westerly) indicate enhanced shear and less tropical cyclone activity, while negative anomalies (easterly) indicate reduced shear and more tropical cyclone activity. Similarly to the Caribbean SLPA, the April and May ZWA are useful as predictors because of their tendency to persist into the heart of the hurricane season. Because of the anomalous circulations forced by ENSO events and the location of the Caribbean stations chosen, the 200-mb ZWA are good measures of the ENSO effect upon the Caribbean and the western North Atlantic (Arkin 1982; Gray 1984a). Table 2 gives the 1950–1991 values of April and May 200-mb ZWA.

El Niño/Southern Oscillation (ENSO). As mentioned earlier, ENSO events cause a large variation in the 200-mb (12 km) circulation over the Caribbean, Gulf of Mexico, and western North Atlantic (Arkin 1982). Gray (1984a) recognized that moderate to strong warm ENSO events reduce the number of Atlantic basin tropical cyclones by creating stronger than normal westerly winds (i.e., more tropospheric vertical wind shear), especially south of 30°N (Shapiro 1987). Additionally, Gray et al. (1993) have included the enhancing effects of moderate to strong cold ENSO events, or La Niñas, toward the predictability of Atlantic basin tropical cyclones. However, while the easterly 200-mb ZWA typically associated with cold ENSO events usually reduce the tropospheric shear and create more favorable conditions for tropical cyclogenesis and intensification, occasionally very strong cold events cause too much *easterly shear* with height and prevent tropical cyclone activity, such as occurred from June to August 1988 (Gray 1988). For forecasting the trop-

ical cyclone activity from 1 June, four predictors are being used that measure the current magnitude of ENSO and its trend. They are the following: the April and May equatorial eastern Pacific SST anomalies (the "Niño 3" region), the change in the SST anomaly from January and February to April and May (Δ_tSST), the April and May SOI, and the change in SOI from January and February to April and May (Δ_tSOI); see Table 2. These provide an indication of what the ENSO conditions will be like during the key August to October time of maximum tropical cyclone activity. Although there is much redundancy between the SST and SOI data, we find that both are necessary to provide the best hindcasts of the seasonal tropical cyclone activity.

b. *West African sea level pressure and temperature gradients*

In a study of multidecadal changes, Hastenrath (1990) identified significant multidecadal trends of July and August sea level pressure and temperature over West Africa and the adjacent Atlantic waters that have coincided with a long-term decrease of Sahel rainfall. In general, over the Atlantic north of 15°N and along coastal West Africa, pressures tended to increase and temperatures tended to decrease from 1948 to 1983. These changes can be attributed to variations in the oceanic "conveyor belt," which has apparently experienced a slowdown in mass and heat transport in the last few decades (Street-Perrott and Perrott 1990). During the same interval in the interior of West Africa, a multidecadal temperature increase and a sea level pressure decrease were observed. These were likely being forced by a feedback of the concurrent persistent trend toward lower rainfall amounts throughout the Sahel region. Similarly, modeling work by Druyan and Koster (1989) showed that there exists a reduced sea level pressure gradient along 15°N from the West African coast to the interior for "rainy" simulations and an enhanced gradient for "drought" simulations (i.e., their Fig. 2) during June and July.

Case study analyses (Lamb 1978; Lamb and Peppler 1992) indicate that the sea surface temperature patterns in the Atlantic that lead to Sahel drought or rainy conditions begin to set up months before the height (August) of the Sahel monsoon. Indeed, the Atlantic sea surface temperature anomalies in April and May are a major portion of the United Kingdom Meteorological Office's real-time empirical and general circulation model (GCM)-based seasonal Sahel forecasts (Folland et al. 1991). Thus, adjacent Atlantic temperature fields have already been shown to be of value in a forecasting mode, and it is likely that coastal station values of temperature and pressure would also be of use for Sahel (and thus tropical cyclone activity) seasonal predictions.

In Fig. 1, linear correlation coefficient patterns of February–May surface temperatures (top panel) and sea level pressures (bottom panel) with IHD* are displayed. This analysis uses individual African and island stations that had a minimum of 15 years of data between 1950 and 1991. Note that in addition to the expected positive temperature–negative pressure correlations along immediate coastal West Africa, a strong pattern of negative temperature–positive pressure correlations occur in interior West Africa south of the Saharan desert. Thus, the use of a difference of the east (interior) and west (coastal) anomalies of temperature and pressure would appear to provide a degree of predictability for upcoming Atlantic tropical cyclone activity, as well as western Sahelian rainfall. A similar use of March and April North African surface temperatures is currently in use for the late May real-time forecasting of the Sahel by the United Kingdom Meteorological Office (Carson 1992). The interior correlations are partly due to the long-term trend of reduced rainfall for the region as seen in the later months of July and August by Hastenrath (1990). However, most of the signal seen cannot be directly related to rainfall trends. It is suggested here that these preseason temperature and pressure patterns set up before the onset of the monsoon and act to alter the strength of the monsoon (as seen in the Sahel rainfall). Figure 2 schematically depicts how these preseason coastal and interior signals can act to alter the Sahel monsoon. A coastal high/cold anomaly coupled with an interior low/warm anomaly forces anomalous surface northeasterlies that weaken the monsoonal southwesterly flow and reduce the Sahel summertime rainfall (and also the Atlantic hurricane activity). Conversely, a coastal low/warm anomaly coupled with an interior high/cold anomaly would lead to anomalous southwesterlies. This would reinforce the monsoonal flow and allow more Sahelian rainfall and Atlantic tropical cyclone activity. These types of anomalous flow patterns and, implicitly, anomalous moisture fluxes, are precisely those described in the modeling work of Folland et al. (1986).

To use these new predictors quantitatively, indices of temperature and sea level pressure were created. All stations within the coastal and interior regions with the minimum 15 years of data for both temperature and sea level pressure were selected (Fig. 3). To make the understanding of the indices as clear as possible, the gradients are set up so that positive February–May east to west anomaly values correspond to above-normal Sahelian rainfall and Atlantic tropical cyclone activity. Thus, $\Delta_x T$ ($T_{\text{coastal}} - T_{\text{interior}}$) is defined as the coastal standardized temperature anomalies minus the interior standardized temperature anomalies, and $\Delta_x P$ ($P_{\text{interior}} - P_{\text{coastal}}$) is defined as interior standardized sea level pressure anomalies minus coastal standardized sea level pressure anomalies. Figures 4a,b show $\Delta_x T$ and $\Delta_x P$ graphically. To provide for a look at potential predictability through $\Delta_x T$ and $\Delta_z P$, Figs. 5a,b show the

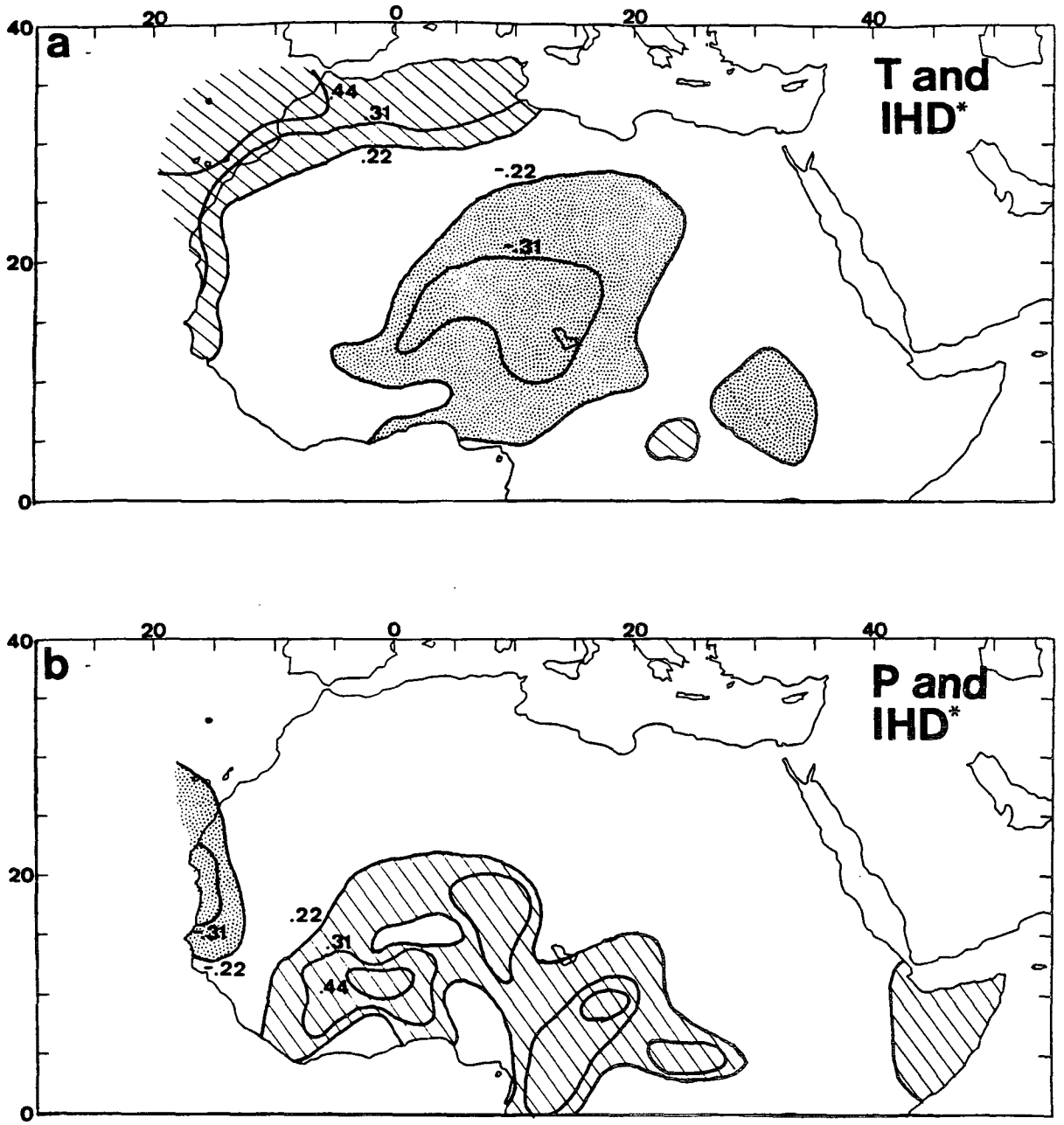

FIG. 1. Linear correlation coefficients of February–May average conditions of (a) surface temperature and (b) sea level pressure with intense hurricane days (IHD*) for the years 1950–1991.

IH* tracks for the ten seasons from 1950 through 1991 with the largest values of $\Delta_x T$ versus those ten seasons with the smallest values of $\Delta_x T$. Figures 6a,b show the same type of information but for $\Delta_x P$. Note the strong modulation of IHD* for both $\Delta_x T$ (a 4.8 to 1 ratio) and $\Delta_x P$ (a 4.5 to 1 ratio).

In summary, the individual effects of the predictors as measured by linear correlation coefficients to various Atlantic basin tropical cyclone measures are shown in Table 3. Note that the strongest predictors are the West African surface data while the weakest tend to be the Caribbean/ENSO data. However, even though the predictors are undoubtedly not independent of one another, the results obtained here and in Gray et al. (1993) indicate that all predictors contribute useful information toward the predictability of Atlantic tropical cyclone activity. We find that when one predictor is combined with another it can often add skill even though, by itself, it may show only very weak predictive ability.

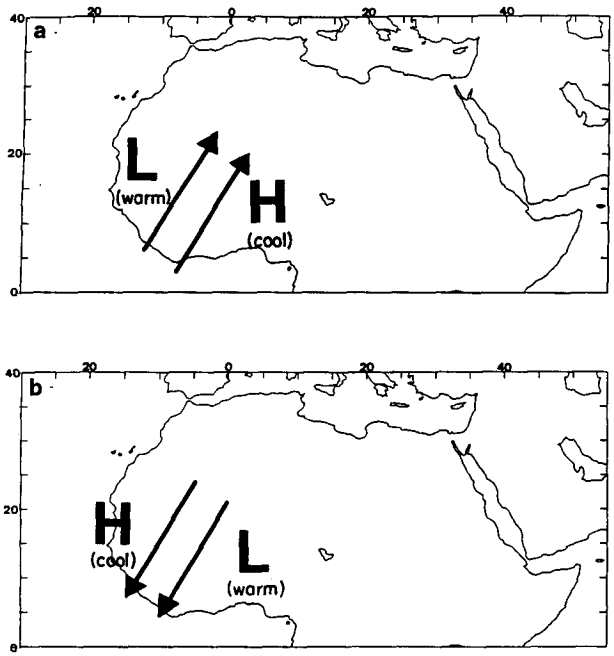

FIG. 2. Schematic of surface pressure anomalies (High-H, or Low-L) and corresponding surface temperature anomalies (a) that enhance (above) and (b) inhibit (below) the summertime West African monsoonal circulation and rainfall.

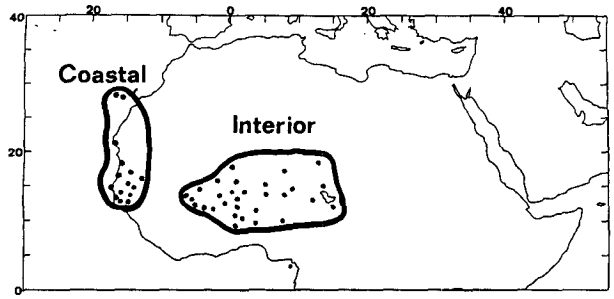

FIG. 3. Station locations for the determination of east to west surface temperature ($\Delta_x T$) and surface pressure ($\Delta_x P$) indices.

3. Analyses and results

The methodology of the statistical procedure has been given in detail in Gray et al. (1992a, 1993). In summary, an objective LAD regression is applied separately to each of the eight dependent variables (NS, NSD, H, HD, IH*, IHD*, HDP*, NTC*) in a cross-validation mode so that each year of data is independently hindcasted. [Note again that the dependent variables marked with an asterisk have been altered from those published in previous reports (Gray et al. 1992a, 1993) because of the small overestimation of intense hurricanes in the 1950s and 1960s as described by Landsea (1993).] This provides us with agreement coefficients (a measure of skill) and probabilities of no relationship. For a forecast of an upcoming season, a procedure without cross validation is performed on all 42 years of the dataset. This leads to a forecast equation in the following form:

$$\hat{y} = \hat{\beta}_0 + \hat{\beta}_1(a_1U_{50} + a_2U_{30} + a_3|U_{50} - U_{30}|) + \hat{\beta}_2(a_4R_s + a_5R_g + a_6\Delta_xP + a_7\Delta_xT) + \hat{\beta}_3(a_8\text{SLPA} + a_9\text{ZWA} + a_{10}\text{SST} + a_{11}\Delta_t\text{SST} + a_{12}\text{SOI} + a_{13}\Delta_t\text{SOI}),$$

where $\hat{y}$ represents one of the eight dependent variables; $\hat{\beta}_0$, $\hat{\beta}_1$, $\hat{\beta}_2$, and $\hat{\beta}_3$ represent the LAD regression weights determined from the solution without cross validation; and a_1, a_2, a_3, a_4, a_5, a_6, a_7, a_8, a_9, a_{10}, a_{11}, a_{12}, a_{13} are selected constants for each composite function. The composite function of U_{50}, U_{30}, and $|U_{50} - U_{30}|$ involves

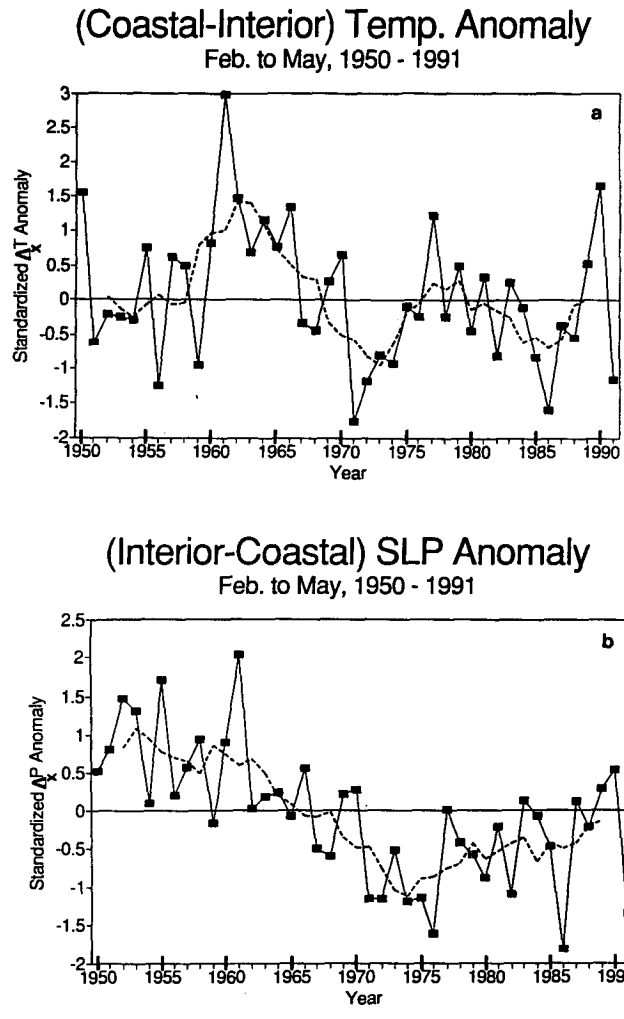

FIG. 4. The 1950–1991 time series of the (a) February–May east to west surface temperature gradient ($\Delta_x T$) and the (b) February–May east to west surface pressure gradient ($\Delta_x P$). The dashed line indicates a five-year running mean.

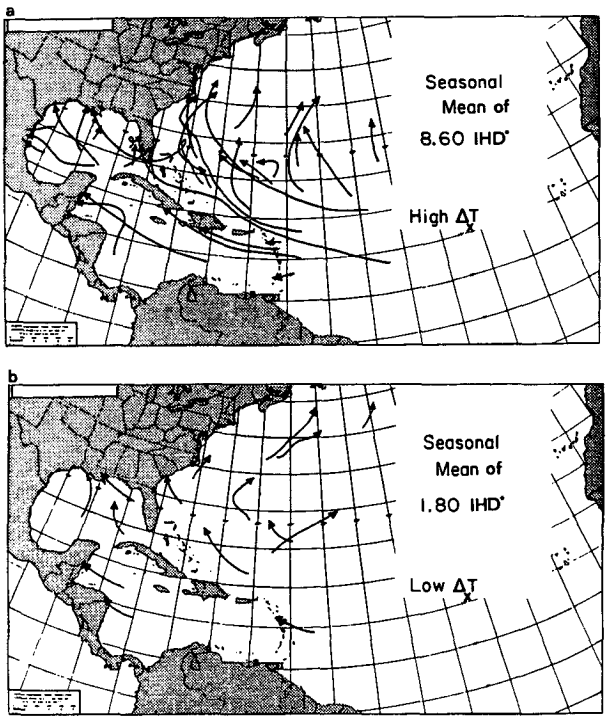

FIG. 5. Contrast of observed IH* tracks for the years 1950–1991 in which the February–May $\Delta_x T$ had the ten highest (a) versus the ten lowest (b) values. The IHD* ratio of this difference is 4.8 to 1.

the stratospheric QBO information. Likewise, the composite function of R_s, R_g, $\Delta_x P$, and $\Delta_x T$ involves the future strength of the western Sahelian monsoon. Last, the composite function of SLPA, ZWA, SST, Δ_tSST, SOI, and Δ_tSOI characterizes Caribbean and ENSO information. Note that the use of the groupings (composite functions) effectively reduces the total number of predictors from 13 to 3. Table 4 presents the values determined for the (a's) and ($\hat{\beta}$'s).

A step-by-step explication of the methodology for constructing the Atlantic basin tropical cyclone activity annual prediction follows. For any prediction the data at hand consist of values for each of the $r = 13$ predictor variables for each of the $n = 42$ years, plus values for each of the eight dependent variables for each of the 42 years. For these purposes we will consider only one dependent variable (number of hurricanes, H) but the same logic applies to the remaining seven dependent variables. The first step in the procedure is to determine cross-validated weights (a's) for each of the 13 independent variables. The cross-validated weights should provide high agreement between the predicted values ($\tilde{y}_i$) and the observed values (y_i) for $i = 1, \cdots, n = 42$. Also, the weights should be obtained in a manner that is completely independent of the known information for a particular year (i.e., the 13 independent variables values and the dependent variable value). This is accomplished through a cross-validation procedure where the hindcast prediction for any year (say, 1964) is based on information obtained from the remaining $n - 1 = 41$ years, and absolutely no information from 1964 is used in the prediction—that is, no information from the 13 independent variables for 1964 and no information from the dependent variable (H) for 1964. This procedure ensures that the cross-validated estimate of y_i ($\tilde{y}_i$) is independent of the data for the year being predicted. An iterative procedure is employed to obtain these cross-validated weights. First, an arbitrary set of $r = 13$ weights (a's) is created. This could be (and has been) as simple as setting $a_1 = \cdots = a_{13} = 1.0$, but it is much more efficient to employ initial values closer to the desired outcomes. For this purpose, the entire $n = 42$ years are used (not cross validated) in a LAD regression with $r = 13$ predictors and these non-cross-validated LAD regression coefficients become the initial starting weights (a's). Then, through a trial-and-error process, the initial weights (a's) are fine-tuned to increase the agreement measure (i.e., decrease the sum of absolute differences) between the $\tilde{y}_i$ and y_i values. This is accomplished by incrementing and decrementing each of the 13 cross-validated weights by very small amounts, running another cross-validated analysis after each change, and comparing the predicted $\tilde{y}_i$ values with the observed y_i values for each of the $n = 42$ years. A measure of agreement ρ is used to determine how close the paired $\tilde{y}_i$ and y_i values are to one another. When $\rho = 1$, then $\tilde{y}_i$

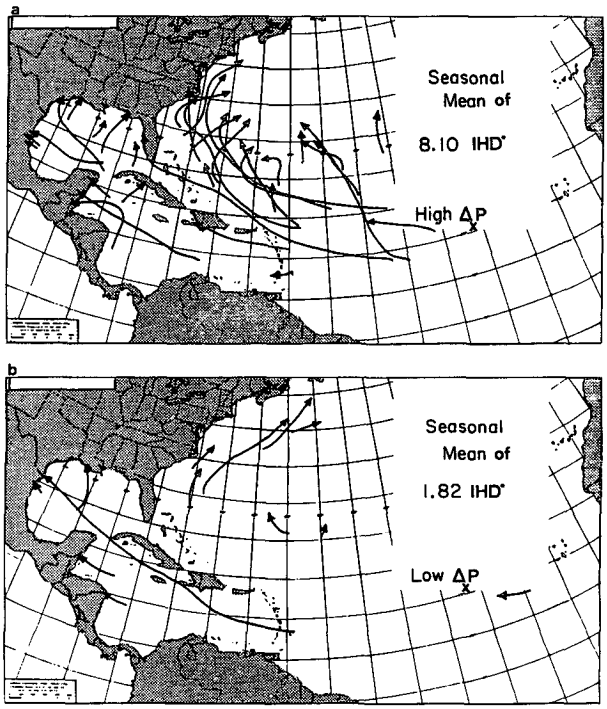

FIG. 6. Same as Fig. 5 but for $\Delta_x P$. The IHD* ratio of this difference is 4.5 to 1.

TABLE 3. Linear correlation coefficients (r) for each of the eight measures of seasonal TC activity with each of the 13 seasonal predictors. Note that other results are presented as r^2 or ρ.

		NS	NSD	H	HD	IH*	IHD*	HDP*	NTC*
QBO	U_{50}	0.45	0.45	0.37	0.38	0.40	0.25	0.37	0.41
	U_{30}	0.38	0.37	0.33	0.31	0.24	0.09	0.26	0.28
	$\lvert U_{50} - U_{30}\rvert$	−0.51	−0.49	−0.53	−0.48	−0.32	−0.23	−0.41	−0.44
AFRICA	R_s	0.00	0.12	0.10	0.23	0.10	0.22	0.23	0.18
	R_g	0.51	0.61	0.58	0.60	0.69	0.60	0.64	0.70
	$\Delta_x P$	0.35	0.44	0.37	0.44	0.55	0.61	0.50	0.57
	$\Delta_x T$	0.19	0.38	0.32	0.47	0.48	0.57	0.50	0.51
Caribbean and	SLPA	−0.14	−0.12	−0.18	0.00	−0.07	0.08	0.00	−0.04
ENSO	ZWA	−0.38	−0.23	−0.30	−0.18	−0.22	−0.18	−0.19	−0.26
	SST	−0.22	−0.24	−0.22	−0.31	−0.29	−0.28	−0.31	−0.31
	Δ_tSST	−0.11	0.00	−0.07	0.00	−0.23	−0.12	−0.05	−0.12
	SOI	0.23	0.23	0.20	0.28	0.24	0.27	0.26	0.29
	Δ_tSOI	0.22	0.04	0.11	0.00	0.16	0.05	−0.01	0.10

$= y_i$ for $i = 1, \cdots, n$ (i.e., a set of perfect hindcasts). Thus, $\rho = 1$ implies a regression line with a zero intercept and a unit slope, which is a special case of linearity. At some point the process stabilizes and no further improvement in the cross-validated agreement coefficient can be accomplished. This does not mean that the model cannot be improved, simply that the agreement coefficient is stable. At this point in the process the cross-validated weights (α's) have been determined for each of the 13 independent variables.

At the next step the 13 independent variables are combined into a smaller number of predictors, each of which is a predictive index of some closely related meteorological phenomena; that is, U_{50}, U_{30}, and the absolute shear between the two levels $\lvert U_{50} - U_{30}\rvert$ compose the predictive index of QBO; two indicators

TABLE 4. Regression weights for the LAD regression procedure prediction equations without cross validation (the β's). Empirical weights for composite functions of QBO, African surface data, and Caribbean/ENSO for the cross-validated LAD regression equations (the a's).

	β_0	β_1	β_2	β_3
NS	12.3781	0.1651	0.6312	−0.2714
NSD	68.8556	1.0409	0.7985	−19.5133
H	9.7544	0.1389	0.5074	−2.5884
HD	41.2690	0.6513	3.8807	−13.1287
IH*	2.5199	0.0252	−0.4059	0.0187
IHD*	6.3386	0.1527	−1.6019	−1.0636
HDP*	112.9477	1.5122	8.5714	−34.8274
NTC*	146.7669	2.0802	−2.2472	−17.0237

	NS	NSD	H	HD	IH*	IHD*	HDP*	NTC*
QBO								
a_1	1.0000	1.0000	1.0000	1.0000	1.0000	1.0000	1.0000	1.0000
a_2	−0.0714	−0.0729	−0.3662	−0.3971	0.4160	−0.2182	−0.3153	−0.1021
a_3	−0.9199	−1.2538	−2.1072	−2.0173	0.2899	−0.7551	−1.8143	−1.1884
AFRICA								
a_4	1.0000	1.0000	1.0000	1.0000	1.0000	1.0000	1.0000	1.0000
a_5	2.4308	8.4673	0.5335	0.5796	−2.4883	−1.0317	1.3122	−7.7489
a_6	−0.0478	1.0972	−1.3485	−0.4836	−2.4395	−1.6112	0.2809	−5.4734
a_7	−0.6367	7.2463	0.8690	1.4982	−0.6668	−0.9943	2.7448	−9.3565
ENSO								
a_8	1.0000	1.0000	1.0000	1.0000	1.0000	1.0000	1.0000	1.0000
a_9	−0.1987	−0.0294	0.0667	−0.0667	5.8344	−0.6537	−0.0889	−0.0824
a_{10}	0.0713	0.0054	−0.0012	−0.0055	−0.6297	0.0103	−0.0016	0.0098
a_{11}	−0.0430	0.0002	0.0016	0.0113	0.0171	0.0167	0.0088	0.0024
a_{12}	0.7902	−0.0037	−0.0521	−0.1327	−1.4853	−0.1748	−0.1166	−0.0687
a_{13}	−0.4711	0.0437	0.0631	0.1258	0.1546	0.2521	0.1199	0.1416

TABLE 5. Agreement coefficient ρ, probability P of no relationship, and r^2 values from a cross-validated LAD regression procedure for the 1 June hindcasts.

	ρ	P	r^2
NS	0.514	0.70×10^{-7}	0.425
NSD	0.660	0.46×10^{-10}	0.688
H	0.617	0.10×10^{-8}	0.595
HD	0.703	0.46×10^{-11}	0.736
IH*	0.637	0.34×10^{-8}	0.703
IHD*	0.614	0.38×10^{-8}	0.654
HDP*	0.709	0.60×10^{-11}	0.751
NTC*	0.718	0.27×10^{-10}	0.760

TABLE 6. Example of year-to-year verification of the forecast of intense hurricane days.

Year	Forecast	Verification	Residual (Forecast − Verification)
1950	15.44	15.75	−0.31
1951	5.00	5.00	0.00
1952	3.75	3.75	0.00
1953	5.50	5.50	0.00
1954	3.88	8.50	−4.62
1955	13.75	13.75	0.00
1956	2.50	2.25	0.25
1957	5.25	5.25	0.00
1958	3.60	8.25	−4.65
1959	−4.64	3.75	−8.39
1960	4.50	10.75	−6.25
1961	14.86	20.75	5.89
1962	3.18	0.00	3.18
1963	5.50	5.50	0.00
1964	11.22	9.75	1.47
1965	3.07	6.25	−3.18
1966	7.00	7.00	0.00
1967	5.82	3.25	2.57
1968	0.00	0.00	0.00
1969	5.17	2.75	2.42
1970	1.51	1.00	0.51
1971	1.32	1.00	0.32
1972	4.40	0.00	4.40
1973	2.50	2.50	0.00
1974	5.01	4.25	0.76
1975	1.67	2.25	−0.58
1976	1.00	1.00	0.00
1977	6.59	1.00	5.59
1978	0.88	3.50	−2.62
1979	2.32	5.75	−3.43
1980	5.48	7.25	−1.77
1981	6.93	3.75	3.18
1982	−0.75	1.25	−2.00
1983	0.25	0.25	0.00
1984	0.75	0.75	0.00
1985	5.14	4.00	1.14
1986	−0.95	0.00	−0.95
1987	0.50	0.50	0.00
1988	7.46	8.00	−0.54
1989	6.36	10.75	−4.39
1990	5.09	1.00	4.09
1991	1.25	1.25	0.00

of western African rainfall (R_g and R_s) and two indicators of western-African pressure and temperature gradient anomalies ($\Delta_x P$ and $\Delta_x T$) compose the predictive index of West African surface data (AFRICA); and Caribbean basin sea level pressure anomalies (SLPA), Caribbean basin 200-mb zonal wind anomalies (ZWA), and four indicators of the current magnitude of ENSO (SST, Δ_tSST, SOI, and Δ_tSOI) compose the predictive index of ENSO. The choice of which independent variables are combined into the predictive indices appears to be arbitrary; however, convenient combinations consist of related meteorological phenomena. Next, one final LAD regression equation is constructed. This last analysis of the data is not cross validated, because it will be used to predict a year into the future—that is, year $n + 1$. The 13 cross-validated weights (a's) based on the final cross-validated analysis are used and all $n = 42$ years are included. This last analysis yields four LAD regression index weights ($\hat{\beta}$'s) from a non-cross-validated solution, one for each of the three predictive indices (QBO, AFRICA, and ENSO) plus a constant. At this point the regression equation is composed of 13 cross-validated weights (a's) and four LAD regression index weights ($\hat{\beta}$'s) and is based on all $n = 42$ years.

Finally, the prediction of the number of hurricanes for year $n + 1$ is made. A LAD regression equation is constructed for the observed values of the 13 predictor

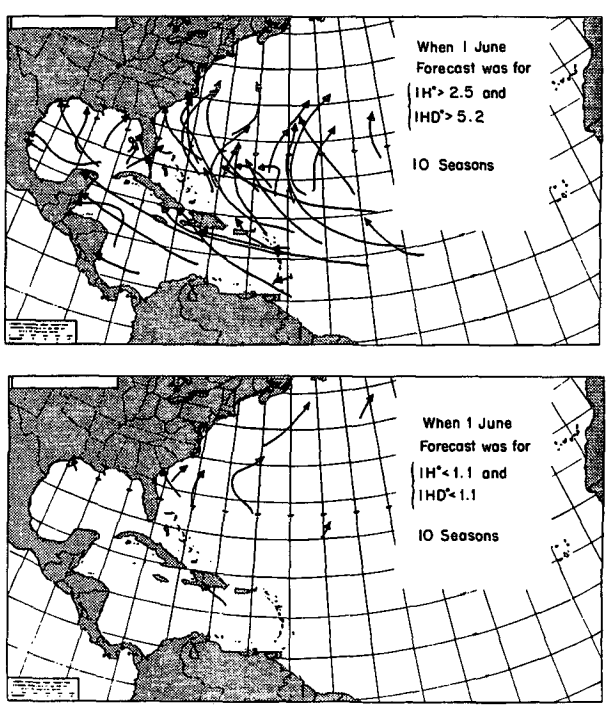

FIG. 7. Contrast of observed IH* tracks between 1950 and 1991 from the ten most active hindcast (IH* > 2.5 and IHD* > 5.2) seasons versus the ten calmest hindcast seasons (IH* < 1.1 and IHD* < 1.1). The IHD* ratio of this difference is 12.9 to 1.

variables (U_{50}, U_{30}, R_g, etc.) for year $n + 1$, and a non-cross-validated prediction value ($\hat{y}$) is made for the number of hurricanes. This entire process is then repeated for the remaining seven dependent variables. The model structure of the 13 predictors is the same for all eight dependent variables, where the (a's) and ($\hat{\beta}$'s) will differ for each dependent variable. It is possible to obtain an improved prediction for a specific dependent variable by constructing a distinct linear (or nonlinear) model for each dependent variable. However, this defeats the goal of using a common prediction model for each of the eight indicators of Atlantic basin tropical cyclone activity.

With this methodology applied to the various predictors described above, we can by 1 June independently hindcast over 60% of the variability (as measured by the agreement coefficient) for all but one (NS) of the eight dependent variables as seen in Table 5. It is extraordinary that we are able to hindcast as much as 70.3% of the variability in HD, 70.9% in HDP*, and 71.8% in NTC*. This appears to be a very powerful forecast technique. The probability of no hindcast statistical skill in any of these predictant variables is between 10^{-7} and 10^{-12}. Table 6 gives an example of the year-to-year forecast and verification of intense hurricane days. Some years, such as, 1959, 1960, 1961, and 1977, the forecast missed the number of intense hurricane days by more than 5. However, in most years there was appreciable skill.

4. Discussion

This paper has presented evidence for a skillful forecast of Atlantic basin tropical cyclone activity by 1 June using information of the future state of the stratospheric QBO, West Africa surface data, and Caribbean/ENSO data. Figure 7 helps to demonstrate the potential skill available in 1 June forecasting by comparing the results of the ten hindcasts for years having highest tropical cyclone activity with the results of the ten hindcasts for the years having lowest tropical cyclone activity. Note the vast difference in observed IH* activity between the active and calm hindcasts. Obviously, if future forecasts are as skillful as the hindcasts suggest themselves to be, then by 1 June, at the "official" start of the hurricane season in the Atlantic basin, it may be possible to forecast nearly three-quarters of the variability of upcoming tropical cyclone activity by the method described in this paper.

Previous work by the authors has focused upon seasonal forecasting of Atlantic tropical cyclone activity by 1 December of the previous year (Gray et al. 1992a) and by 1 August of the current year (Gray et al. 1993). Because of the analyses of Landsea (1993), a reworking of the results of Gray et al. (1992a, 1993) was in order. Table 7 presents the revised constants for 1 December of the previous year and 1 August of the current year forecasts of IH*, IHD*, HDP*, and NTC*. These revisions resulted in either no change or only a small

TABLE 7. Same as Table 4 for revised IH*, IHD*, HDP*, and NTC* for 1 December of the previous year forecast (Gray et al. 1992a) and for 1 August of the current year forecast (Gray et al. 1993).

	1 December			1 August			
	β_0	β_1	β_2	β_0	β_1	β_2	β_3
IH*	2.7590	0.0316	0.3592	2.9998	0.0134	0.7450	−0.2895
IHD*	6.4086	0.0381	1.1286	4.8060	0.1085	4.9325	−0.5685
HDP*	86.6214	0.4572	18.9744	85.8351	1.6154	30.9894	−4.0380
NTC*	123.6108	0.4534	17.7062	122.8190	1.4805	11.3101	−0.6185

	IH*	IHD*	HDP*	NTC*
		1 December		
a_1	1.0000	1.0000	1.0000	1.0000
a_2	−0.0146	−1.9858	1.7780	1.8000
a_3	−1.1649	−7.4296	−1.2600	−2.4990
a_4	1.0000	1.0000	1.0000	1.0000
a_5	3.7987	3.8304	2.1180	2.8690
		1 August		
a_1	1.0000	1.0000	1.0000	1.0000
a_2	2.4483	0.1953	0.5501	1.0556
a_3	−0.8757	0.9289	0.6494	1.0129
a_4	1.0000	1.0000	1.0000	1.0000
a_5	0.6891	0.2220	0.1864	1.8147
a_6	1.0000	1.0000	1.0000	1.0000
a_7	0.1660	0.2863	0.4966	1.7093
a_8	0.4763	3.0452	1.9775	13.7971
a_9	1.4624	1.2702	3.3274	21.7751

TABLE 8. Comparison of hindcast skill measured by agreement coefficient for previous work based on differing forecast starting points. Note that the IH*, IHD*, HDP*, and NTC* have been recalculated to adjust for the small bias in the 1950–1969 tropical cyclone data found by Landsea (1993).

	1 June of current year	1 December of previous year (Gray et al. 1992a)	1 August of current year (Gray et al. 1993)
NS	0.514	0.440	0.477
NSD	0.660	0.514	0.608
H	0.617	0.447	0.472
HD	0.703	0.491	0.505
IH*	0.637	0.465	0.586
IHD*	0.614	0.452	0.540
HDP*	0.709	0.444	0.549
NTC*	0.718	0.532	0.581

reduction in hindcast skill. Table 8 details these variations in skill as measured in agreement coefficients for each of the three forecasting starting dates. Note that the current work shows by far the most skill for all eight dependent variables.

Acknowledgments. The authors wish to thank Richard Taft and William Thorson for their programming and data processing assistance, and to John Sheaffer, John Knaff, Pat Fitzpatrick, and Ray Zehr for providing many beneficial discussions. Barbara Brumit and Laneigh Walters provided expert manuscript assistance. Richard Tinker of the Climate Analysis Center, Tom Ross of the National Climatic Data Center, and Colin McAdie of the National Hurricane Center have all been very helpful in providing near real-time temperature, pressure, precipitation, and wind data. We also wish to thank Lloyd Shapiro and two anonymous reviewers for their helpful critiques of the earlier version of this paper. This research was supported by a climate grant from the National Science Foundation and by a special supplementary grant by the NOAA National Weather Service.

REFERENCES

Arkin, P. A., 1982: The relationship between the interannual variability in the 200 mb tropical wind field and the Southern Oscillation. *Mon. Wea. Rev.*, **110,** 1393–1401.

Brennan, J. F., 1935: Relation of May–June weather conditions in Jamaica to the Caribbean tropical disturbances of the following season. *Mon. Wea. Rev.*, **63,** 13–14.

Carson, D. J., 1992: Preliminary experimental forecast of 1992 seasonal rainfall in the Sahel and other regions of tropical North Africa. Unpublished report, 3 pp. [Available from the National Meteorological Library, Meteorological Office, Bracknell, Berkshire, United Kingdom.]

Druyan, L. M., and R. D. Koster, 1989: Sources of Sahel precipitation for simulated drought and rainy seasons. *J. Climate,* **2,** 1438–1446.

Folland, C. K., T. N. Palmer, and D. E. Parker, 1986: Sahelian rainfall and worldwide sea temperatures 1901–1985. *Nature,* **320,** 602–607.

——, J. A. Owen, M. N. Ward, and A. W. Colman, 1991: Prediction of seasonal rainfall in the Sahel region using empirical and dynamical methods. *J. Forecasting,* **10,** 21–56.

Goldenberg, S. B., and L. J. Shapiro, 1993: Relationships between tropical climate and interannual variability of North Atlantic tropical cyclones. Preprints, *20th Conf. on Hurricanes and Tropical Meteorology,* San Antonio, TX, Amer. Meteor. Soc., 102–105.

Gray, W. M., 1968: Global view of the origins of tropical disturbances and storms. *Mon. Wea. Rev.*, **96,** 669–700.

——, 1984a: Atlantic seasonal hurricane frequency. Part I: El Niño and 30 mb quasi-biennial oscillation influences. *Mon. Wea. Rev.*, **112,** 1649–1668.

——, 1984b: Atlantic seasonal hurricane frequency. Part II: Forecasting its variability. *Mon. Wea. Rev.*, **112,** 1669–1683.

——, 1988: Summary of 1988 Atlantic tropical cyclone activity and verification of author's seasonal forecast. Colorado State University, Department of Atmospheric Sciences Paper, Ft. Collins, CO, 49 pp.

——, 1990: Strong association between West African rainfall and U.S. landfall of intense hurricanes. *Science,* **249,** 1251–1256.

——, C. W. Landsea, P. W. Mielke, and K. J. Berry, 1992a: Predicting Atlantic seasonal hurricane activity 6–11 months in advance. *Wea. Forecasting,* **7,** 440–455.

——, J. D. Sheaffer, and J. A. Knaff, 1992b: Influence of the stratospheric QBO on ENSO variability. *J. Meteor. Soc. Japan,* **70,** 975–995.

——, C. W. Landsea, P. W. Mielke, and K. J. Berry, 1993: Predicting Atlantic seasonal tropical cyclone activity by 1 August. *Wea. Forecasting,* **8,** 73–86.

Hastenrath, S., 1990: Decadal-scale changes of the circulation in the tropical Atlantic sector associated with Sahel drought. *Int. J. Climatol.*, **10,** 459–472.

Jarvinen, B. R., C. J. Neumann, and M. A. S. Davis, 1984: A tropical cyclone data tape for the North Atlantic basin, 1886–1983: Contents, limitations, and uses. NOAA Tech. Memo. NWS NHC 22, Miami, FL, 21 pp.

Knaff, J. A., 1993: Evidence of a stratospheric QBO modulation of tropical convection. Atmospheric Sciences Paper No. 520, Colorado State University, Ft. Collins, CO, 91 pp.

Lamb, P. J., 1978: Large-scale tropical Atlantic surface circulation patterns associated with Subsaharan weather anomalies. *Tellus,* **A30,** 240–251.

——, and R. A. Peppler, 1992: Further case studies of tropical Atlantic surface atmospheric and oceanic patterns associated with Subsaharan drought. *J. Climate,* **5,** 476–488.

Landsea, C. W., 1993: A climatology of intense (or major) Atlantic hurricanes. *Mon. Wea. Rev.*, **121,** 1703–1713.

——, and W. M. Gray, 1992: The strong association between western Sahel monsoon rainfall and intense Atlantic hurricanes. *J. Climate,* **5,** 435–453.

——, ——, P. W. Mielke, and K. J. Berry, 1992: Long-term variations of western Sahelian monsoon rainfall and intense US landfalling hurricanes. *J. Climate,* **5,** 1528–1534.

Neumann, C. J., B. R. Jarvinen, A. C. Pike, and J. D. Elms, 1987: *Tropical Cyclones of the North Atlantic Ocean, 1871–1986.* National Climatic Data Center in cooperation with the National Hurricane Center, 186 pp.

Nicholson, S. E., 1979: Revised rainfall series for the West African subtropics. *Mon. Wea. Rev.*, **107,** 620–623.

Ray, C. L., 1935: Relation of tropical cyclone frequency to summer pressures and ocean surface-water temperatures. *Mon. Wea. Rev.*, **63,** 10–12.

Shapiro, L. J., 1982: Hurricane climate fluctuations. Part II: Relation to large-scale circulation. *Mon. Wea. Rev.*, **110,** 1014–1023.

——, 1987: Month-to-month variability of the Atlantic tropical circulation and its relationship to tropical storm formation. *Mon. Wea. Rev.*, **115,** 2598–2614.

——, 1989: The relationship of the quasi-biennial oscillation to Atlantic tropical storm activity. *Mon. Wea. Rev.*, **117,** 1545–1552.

Street-Perrott, F. A., and R. A. Perrott, 1990: Abrupt climate fluctuations in the tropics: The influence of the Atlantic circulation. *Nature,* **343,** 607–612.